

# Transient Dynamics of Pinning

G. K. Leaf,<sup>1</sup> S. Obukhov,<sup>2</sup> S. Scheidl,<sup>3</sup> and V. M. Vinokur<sup>4</sup>

<sup>1</sup>Mathematics and Computer Science Division, Argonne National Laboratory, Argonne, IL 60439

<sup>2</sup>University of Florida, Gainesville, FL 32611

<sup>3</sup>Institut für Theoretische Physik, Universität zu Köln, Zulpicher Str. 77, D-50937 Köln, Germany

<sup>4</sup>Materials Science Division, Argonne National Laboratory, Argonne, IL 60439

(April 14, 2024)

We study the evolution of an elastic string into the pinned state at driving forces slightly below the depinning threshold force  $F_c$ . We quantify the temporal evolution of the string by an activity function  $A(t)$  representing the fraction of active nodes at time  $t$  and find three distinct dynamic regimes. There is an initial stage of fast decay of the activity; in the second, intermediate, regime, an exponential decay of activity is observed; and, eventually, the fast collapse of the string towards its nally pinned state results in a decay in the activity with  $A \sim (t_p - t)^{-1}$ , where  $t_p$  is the pinning time in the finite system involved.

Driven dynamics of disordered elastic media, which has become a paradigm for a diversity of physical systems, is characterized by the existence of a depinning force  $F_c$ , which separates the pinned state at "sub-threshold" forces  $F < F_c$  and the sliding regime at "super-threshold" forces  $F > F_c$ . At finite temperatures the system can move at sub-threshold forces as a result of thermally activated jumps between the disorder-induced meta-stable states. The corresponding activation barriers diverge at small forces,  $U(F) \sim 1/F \rightarrow 0$ , giving rise to glassy dynamics with a highly nonlinear response to infinitesimal drives [1,3] (creep), aging, memory, and hysteretic effects [4,7]. On the qualitative phenomenological level, the observed memory and hysteretic behaviors can be viewed as a result of slow relaxation of the relevant activation barriers upon altering the drive [8], yet the detailed quantitative description of transient glassy dynamics remains an appealing task. The static sub-threshold characteristics of the string were studied in [9] and critical depinning and transient behavior in the sliding regime in [10]. In this letter we investigate numerically and analytically the transient sub-threshold zero-temperature dynamics of an elastic string, taken as an exemplary system for a driven elastic disordered medium. We study the time evolution of the string as it slows and eventually stops upon applying a constant driving force in the vicinity of the depinning threshold,  $F < F_c$ , where the transient period and the distance traveled by the string are large and diverge as  $F \rightarrow F_c$ .

The graphic representation of a typical time evolution of the string velocity  $v(x;t)$  is given in Fig. 1. It demonstrates the avalanche-like sub-threshold dynamics of the string. The avalanches advance via the propagation of kinks along the string. We quantify the temporal evolution by the activity function  $A(t)$  defined as the fraction of the moving nodes at time  $t$ , which is proportional to the velocity of the center of mass of the string [11], and find three distinct regimes of the temporal evolution of

the string: (i) an initial regime of a fast decay of activity, according to a power law; (ii) the exponential decay of activity,  $A \sim \exp[-(t-t_p)]$  and (iii) the final avalanche-like immobilization stage, which appears only for strings of finite length for which the activity vanishes and the string gets pinned at a finite time  $t_p$ . Shortly before  $t_p$  the activity function drops rapidly to zero following the power law,  $A \sim (t_p - t)^{-1}$ , with  $0.63$ .

Model { We consider an elastic string at zero temperature placed on a disordered plane and subject to a constant drive  $F$  not exceeding the critical depinning force  $F_c$ . The overdamped equation of motion is  $\partial y / \partial t =$

$H = \eta y$ , where  $y(x;t)$  is its lateral displacement at time  $t$ ,  $\eta$  is a friction coefficient. The string has a length  $L$  and is aligned along the  $x$  direction. Its energy is

$$H = \int_0^L dx \left[ \frac{C}{2} \left( \frac{\partial y}{\partial x} \right)^2 + U(y(x);x) \right];$$

with the string elastic constant  $C$ . The string and the media are periodic in  $x$  with periodicity  $L$ .

In the simulations we use a discrete version of the continuum equations. The  $x$  direction is discretized by a set of lines (rails) of equal spacing, with unit length, constraining the motion of discrete string elements (nodes). Energies are measured in the units of the elastic constant  $C$ . The pinning sites are randomly distributed on the rails according to a specified density  $\rho = 0.1$ . The pinning sites are triangular wells with unit width and the depth/strength  $U_p = 0.1$ . Forward Euler time marching is used to advance the system in time. The initial state for the string is taken as a straight line. The statistics were collected on 30 samples of length  $L = 8192$ .

Results { To link to past research, we measured the geometric characteristics of the subthreshold behavior. The roughness of the string at time  $t$  is  $w_t(x) = \sqrt{\langle [y(x;t) - y(x^0;t)]^2 \rangle^{1/2}}$ , where  $\langle \cdot \rangle$  denotes a positional average over  $x^0$  and a disorder average. The roughness increases with  $x$  (for  $x \ll L$ ) until it saturates at  $x \sim L$  ( $t$ )

with  $w_t(x) \sim \tau(t)$  (see Fig. 2). Correlation lengths increase with time and reach the final values  $\xi_k$  and  $\xi_\tau$  in the pinned state ( $t \gg t_p$ ), where the roughness follows a power law  $w_1 \sim x$  for  $1 \leq x \leq \xi_k$  [12]. We find the roughening exponent to grow linearly as the applied force approaches its threshold value  $F_c$  (see inset of Fig. 3). This behavior allows for an alternative determination of  $F_c$  resting on the analytical estimate  $\alpha = 1$  at the transition [13]. This contrasts with the usual procedure where two parameters  $F_c$  and  $\alpha$  have to be simultaneously determined as fitting parameters. The criterion  $\alpha(F_c) = 1$  yields as an estimate for the critical depinning force  $F_c = 0.3016$ , which is in excellent agreement with our value of the critical force determined independently from the double-logarithmic plot of roughness ( $F_c = 0.3105$ ) and also with the earlier finding [14] ( $F_c = 0.3058$ ). Note a discrepancy with the results in Ref. [10], where  $\alpha = 1.25$  at the depinning transition has been found in conflict with the analytical result of [13]. The reason for this discrepancy is not yet clear.

Next, we studied the behavior of the pinning distance  $[9] D_p$ , which is defined as the ensemble averaged distance that the center of mass of the string traveled before being completely pinned  $D_p = (1/L) \sum_{i=1}^L y_i(t_p) - y_i(0)$ . We verified the scaling behavior of  $D_p \sim (F - F_c)^{-1}$  (cf. Fig. 3). For the given string length  $L = 8192$  the finite-size effects become negligible for the force dependence. We found  $\alpha = 2.56 \pm 0.08$  for  $F_c = 0.3016$  in good agreement with the results of [9] for the 1D CDW. The other relevant quantities  $\xi_k$  and  $\xi_\tau$ , determined from the saturation of the roughness also scale with exponents grouping around  $\alpha = 2.4$ . The results are summarized in the Table I, which also gives the values of the critical force determined independently from the divergences of the quantities involved.

Having established the geometric characteristics of subthreshold dynamics, we now turn to a detailed study of the temporal evolution of transient behavior. We characterize the temporal evolution of a finite system toward the pinned state by the activity function  $A(t)$  defined as the fraction of the moving string nodes moving at the given instant  $t$ . For a discrete system evolving in time by steps  $\tau$ , we define a node as active at time  $t$  if that node has moved at least one lattice unit in the previous 100 time steps. The activity function is then the ensemble average of the fraction of active nodes. In Fig. 4 we illustrate the temporal behavior of the activity function for the representative subthreshold force  $F = 0.29$ .

It is important to quantify not only the fraction of active nodes, but also the spatial structure of pinned and moving nodes, which can be quantified by the characteristic length  $L_{pin}$  of pinned segments (connected region of pinned nodes). Initially,  $L_{pin}$  will be of the order of unity, since the string position is not correlated with the location of the pinning centers and in the final pinned state  $L_{pin} = L$  (see inset of Fig. 2). The initial

transient regime (i) is expected to last until  $t$  given by  $L_{pin}(t) = \xi_k$  [10].

At  $t > t_p$  relatively large segments of the string are pinned, and the remaining activity is due to the motion of mobile segments over rare regions, where the pinning centers are underrepresented. These mobile segments will advance until the driving force is balanced by other pinning centers or by the string tension. We now construct a lower estimate for the velocity of an infinitely long string as a function of time. We expect the finite string in regime (ii) to follow this dynamics, before finite-size effects set in in regime (iii). We divide the rails in elements of unit length. Then a finite fraction  $p$  of elements is free of a pinning force. We overestimate the effect of pinning by assuming that the other elements contain an infinitely strong pinning force. Let us now consider a string segment that is pinned on two rails of distance  $l$ , say at  $y(0) = y(l) = 0$ . If the rails in between are free of pinning centers, the segment relaxes into the configuration where the driving force is balanced by the string tension. A simple estimate shows that the front of the segment will then reach a distance  $y_1 = F l^2 / C$  after a time  $t_1 = y_1 \frac{C}{F} = \frac{F l^2}{C^2}$ . Before this time the ends of length  $x(t) = \frac{F l^2}{C t}$  of the string segment come to rest, and the center of mass of the segment moves with a velocity  $v_1(t) = \frac{F}{C} [1 - \frac{F l^2}{C t}]$ . During this relaxation the string segment moves over an area  $A_1 = F l^2 / C$ . The relaxation takes place in this undisturbed way only if all the rail segments in this area are free of pinning, which occurs with probability  $p_1 = p^{A_1}$ .

To find a lower bound to the string velocity we divide the whole string into segments of arbitrary length  $l$ , which serves as variational parameter. Although the string can be taken as unpinned initially, the velocity is underestimated by formally considering the links between these sections as pinned. A fraction  $p_1$  of such segments relaxes without encountering pinning rail elements and contributes  $p_1 v_1(t)$  to the average string velocity. This contribution is a lower bound to the velocity for all possible  $l > 0$ , and the best estimate is obtained by  $v_{min}(t) = \max_l p_1 v_1(t) = p^{(F=C)(Ct)^{3/2}}$ , which is finite at all times. Consequently, the activity function is also expected to decay not faster than  $A(t) > \exp(-\text{const} t^{3/2})$ .

In the finite system this exponential decay stops when the characteristic distance between the moving segments  $L_{pin} = l_p$  becomes of the order of the system size and the string experiences a deficiency of the moving nodes. Our conjecture is that the origin of this "superfast" stopping regime is the avalanche-like disappearance of the moving nodes of the string. Once pinned, a node cannot depin any more; moreover, it causes the immediate pinning of the neighboring nodes, in a close analogy with the avalanche clustering at the final stage of the coagulation process [15]. This analogy suggests the power-law termination of the motion according to  $A_r(t_p - t) \sim t^{-j}$ ,

where  $t_p$  is the time of the total immobilization. Although  $t_p$  is subject to strong sample-to-sample fluctuations because it is determined by fluctuations on the scale of the system size, the final regime can be recognized only by averaging the activity considered as a function of the reverse time  $t_p - t$ ; that is, the final regime can be seen only if the averaging over  $N$  samples is performed according to  $A_r(t_p - t) = (1/N) \sum_{i=1}^N A_i(t_p^{(i)} - t)$  in contrast to the usual average  $A(t) = (1/N) \sum_{i=1}^N A_i(t)$ .

We give lower and upper limits on the exponent  $\beta$ . Consider the process in which the node that came to rest enhances the probability that the nearest node will stop at the next moment of time. In this case the boundary between localized and mobile nodes will move some average velocity, and the activity will decrease as  $A_r / (t_p - t)$ , which means that the upper limit on  $\beta$  is  $\beta_{upper} = 1$ . This type of behavior can be expected when  $F$  is far below  $F_c$ . Another limiting type of terminal dynamics occurs if immobile nodes do not affect dynamics in mobile regions. In this case the boundary between the immobile and mobile regions moves randomly, and the finite string has a nonzero chance of stopping when the boundaries enclosing the moving region collide with each other. Considering this process in reverse time, we conclude that  $A_r / (t_p - t)^{1/2}$ , and we get a lower limit  $\beta_{lower} = 1/2$ . Note, that the possibility of fragmentation of the moving segment of the string into several subsegments does not affect this estimate. In the more general case of a moving manifold of internal dimension  $d$  ( $d = 1$  for the string), similar arguments result in  $d/2 < \beta < d$ .

Numerical simulations clearly show distinct relaxation regions. After the initial relaxation (regime (i)), the activity crosses over to the exponential decay regime,  $A(t) \sim \exp[-(t-t_p)]$ ,  $\beta = 1$ . The precision of our data is not sufficient to determine a more precise estimate of  $\beta$ ; from the above consideration we could expect  $1 < \beta < 2$ . The relaxation time  $t$  diverges as the applied force approaches the threshold value (see Fig. 3). However, although one could expect that  $t = t_p$  and therefore that  $t \sim F_c - F$  (since  $F \sim F_j$ ), with  $z = 4/3$  using the exponents of the depinning transition [10], we have found a different exponent:  $t \sim F_c - F$  with  $\beta = 2.74$ . A careful examination of a final stage of the relaxation process reveals a very sharp drop of the activity function just before the complete immobilization of the string. To analyze this stage, we introduce the reverse time representation: we present the activity function as a function of  $t_r = t_p - t$ , counting time backwards from the moment of achieving final immobilization. Using this representation enables us to carry out an ensemble averaging despite the fact that different samples have different pinning times. The plot of  $\ln A_r$  vs.  $\ln(t_p - t)$  reveals a power-law final behavior (see Fig. 5):  $A_r(t_p - t)$ , with  $\beta = 0.63 \pm 0.06$ , which is within the above upper and lower estimates. We note that the

reverse time plot of  $\ln A_r$  confirms the existence of the intermediate regime with the essentially same characteristic time  $t$  as was found from the direct time picture.

In summary, we investigated subthreshold dynamics of a pinned elastic string and identified three distinct transient regimes: (i) a fast initial relaxation, (ii) an intermediate exponential decay of the activity resulting from residual motion in the exponentially rare regions free of defects and (iii) a novel avalanche-like terminal relaxation to the pinned state,  $A_r(t_p - t)$ , resulting from the finite-sized effects. This final stage exhibits striking similarity to coagulation dynamics.

This work was supported by Argonne National Laboratory through the U.S. Department of Energy, BES-Material Sciences and BES-MICS, under contract No. W-31-109-ENG-38, and by the NSF Office of Science and Technology Centers under contract No. DMR91-20000 Science and Technology Center for Superconductivity.

- 
- [1] L.B. Ioé and V.M. Vinokur, J. Phys. C 20, 6149 (1987)
  - [2] G. Blatter et al., Rev. Mod. Phys. 66, 1125 (1994)
  - [3] V.M. Vinokur, M.C. Marchetti, and L.-W. Chen, Phys. Rev. Lett., 77, 1845 (1996)
  - [4] J.A. Fendrich et al., Phys. Rev. Lett. 77, 2073 (1996).
  - [5] W. Henderson, E.Y. Andrei, and M.J. Higgins, Phys. Rev. Lett. 81, 2352 (1998)
  - [6] S.N. Goryunov et al., Nature, 385, 324 (1997)
  - [7] M. Etushko et al., unpublished
  - [8] S. Scheidland V.M. Vinokur, Phys. Rev. Lett. 77, 4768 (1996).
  - [9] A. Middleton and D. Fisher, Phys. Rev. B 47, 3530 (1993)
  - [10] H. Leschhorn et al., Ann. Phys. (Leipzig) 6, 1 (1997).
  - [11] In the subthreshold regime the motion of the string is avalanche-like. Once a bead participates in an avalanche, it reaches a typical maximum velocity that is independent of the time, where the avalanche started. The activity is defined by the fraction of particles with a velocity exceeding a threshold velocity smaller than the typical maximum velocity. Therefore, the activity is proportional to the average velocity.
  - [12] T. Halpin-Healy and Y.-C. Zhang, Physics Reports 254, 215 (1995).
  - [13] O. Narayan and D.S. Fisher, Phys. Rev. B 48, 7030 (1993).
  - [14] M. Dong et al., Phys. Rev. Lett. 70, 662 (1993).
  - [15] M.H. Emsw, Kinetic theory of clustering, in Fundamental problems of statistical mechanics VI, Ed. E.G.D. Cohen, Elsevier Science Publ., B.V. (1985)

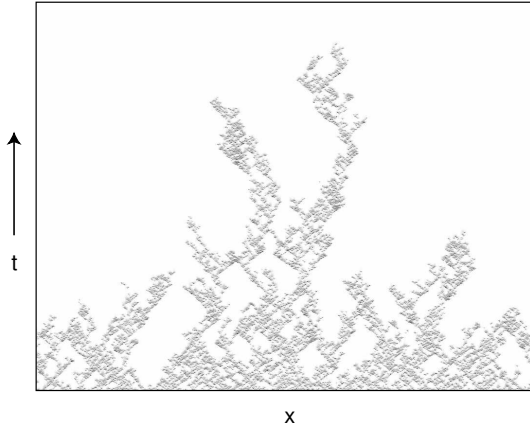


FIG. 1. History of the string velocity (gray-scale plot of  $v(x;t)$  using white for zero velocity and black for large velocity). Note that in the active regions (avalanches) the velocity of the beads reaches the same values at early and late stages of the evolution, which differ only in the number and size of avalanches, which is measured by the activity.

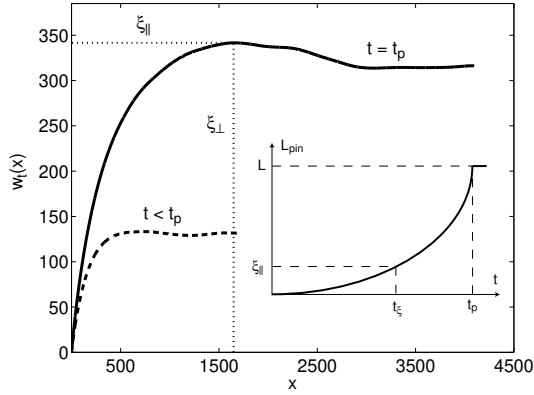


FIG. 2. Plot of the roughness  $w_t(x)$  at intermediate time ( $t < t_p$ , truncated for large  $x$  beyond saturation) at final stage ( $t = t_p$ ), where it saturates on the scale of the correlation lengths  $\xi_{\parallel}$  and  $\xi_{\perp}$ . The nonmonotonic shape of  $w_t(x)$  is an artifact of the finite number of samples used for disorder averaging. Inset: time evolution of the typical size  $L_{pin}$  of pinned string segments.

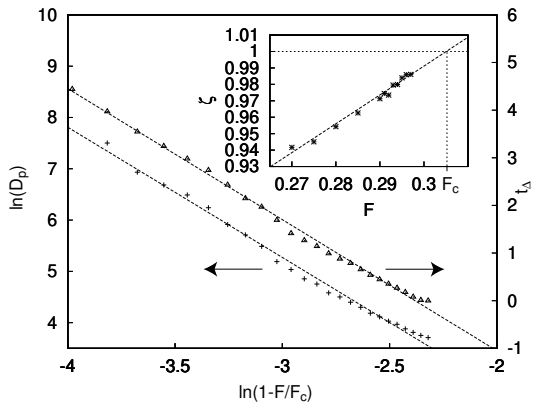


FIG. 3. Inset: The roughening exponent  $\zeta$  as a function of the driving force  $F$  (stars: measured values, dashed line: linear fit), which assumes the value  $\zeta = 1$  at the critical force  $F = F_c$ . Main plot: force dependence of the pinning distance  $D_p$  (crosses) and of the relaxation time  $t$  (triangles) with linear fits (dashed lines) in the double-logarithmic representation.

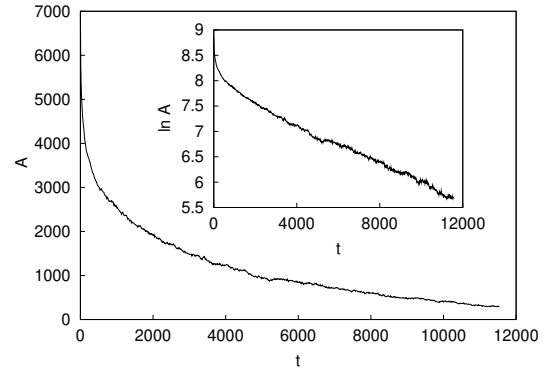


FIG. 4. Time dependence of the activity  $A$  for the force value  $F = 0.29$  in linear and semilogarithmic representation.

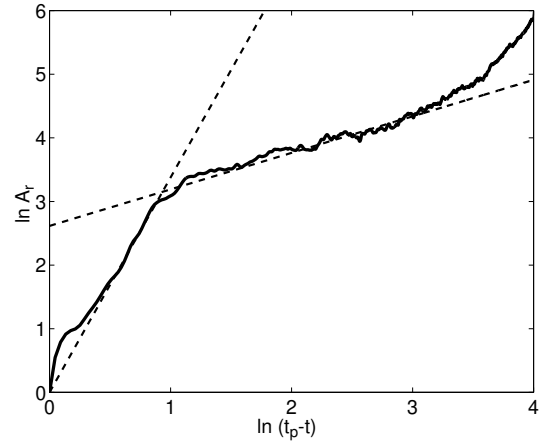


FIG. 5. Plot of the activity  $A_x$  as a function of the reverse time ( $t_p - t$ ). The dashed lines represent linear fits to the regimes (ii) and (iii) introduced in the text.

|       | $D_p$        | $\zeta$      | $\kappa$    |
|-------|--------------|--------------|-------------|
|       | 2.56 0.08    | 2.41 0.07    | 2.38 0.09   |
| $F_c$ | 0.2978 0.001 | 0.3011 0.002 | 0.3007 0.01 |

TABLE I. Values of the scaling exponent  $\zeta$  and the critical force  $F_c$  as determined from the divergences of  $D_p$ ,  $\zeta$ , and  $\kappa$ .